



## Original Article

Synergistic interaction of  $\beta$ -caryophyllene with aromadendrene oxide 2 and phytol induces apoptosis on skin epidermoid cancer cellsP.S. Pavithra<sup>a</sup>, Alka Mehta<sup>a</sup>, Rama S. Verma<sup>b,\*</sup><sup>a</sup> School of Bio Sciences and Technology, Vellore Institute of Technology, Vellore-632 014, India<sup>b</sup> Department of Biotechnology, Bhupat & Jyoti Mehta School of Biosciences, Indian Institute of Technology Madras, Chennai 600 036, India

## ARTICLE INFO

## Keywords:

*P. missionis* $\beta$ -caryophyllene

Aromadendrene oxide 2

Phytol

Synergy

Apoptosis

Cancer therapy

## ABSTRACT

**Background:** *Pamburus missionis* (Wight) Swingle (Rutaceae) is traditionally used in the treatment of swellings, chronic rheumatism, paralysis and puerperal diseases. In a previous study the authors demonstrated apoptotic activity of *Pamburus missionis* essential oil (EO) on A431 and HaCaT cells. The major components of EO were  $\beta$ -caryophyllene (25.40%), 4(14),11- eudesmadiene (7.17%), aromadendrene oxide 2 (14.01%) (AO-(2)) and phytol (6.88%).

**Purpose of study:** To investigate the role as well as the interactions among EO components inducing apoptosis in A431 and HaCaT cells.

**Methods:** Isobolographic analysis and combination index methods were used to detect the type of interactions among the essential oil (EO) components. Cell viability was used to detect cytotoxic activity. Mechanism of cell death was studied using Annexin V-FITC/PI binding assay, cell cycle analysis, measurement of MMP and ROS generation by flow cytometry. Expression of apoptosis associated proteins was investigated by western blot.

**Results:** Combination of *P. missionis* EO components:  $\beta$ -caryophyllene/ aromadendrene oxide 2 ( $\beta$ -C/AO-(2)),  $\beta$ -caryophyllene/phytol ( $\beta$ -C/P) and aromadendrene oxide 2 /phytol (AO-(2)/P) inhibited growth and colony formation ability of skin epidermoid A431 and precancerous HaCaT cells. Synergistic interaction was observed between  $\beta$ -C/AO-(2) and  $\beta$ -C/P combination while AO-(2)/P exhibited an additive effect. Combination of components induced chromatin condensation, phosphatidylserine externalisation, increase in sub-G1 DNA content, cell cycle arrest at G0/G1 phase and intracellular ROS accumulation. Inhibition of intracellular ROS by N-acetyl cysteine treatment blocked apoptosis induced by the combinations. The combinations induced apoptosis in A431 and HaCaT cells mediated by loss of mitochondrial membrane potential ( $\Delta\Psi_m$ ), increase in Bax/Bcl-2 ratio, release of cytosolic cytochrome c and activation of caspases (cleaved form of caspase-3, caspase-8, caspase-9) and by PARP cleavage.

**Conclusion:** The present study demonstrates interactions among  $\beta$ -C, AO-(2) and P in the induction of apoptosis on A431 and HaCaT cells. These data suggest the combination of  $\beta$ -caryophyllene with aromadendrene oxide 2 and phytol could be potential therapeutics for the treatment of skin epidermoid cancer and precancerous cells.

## Introduction

Skin cancers are by far the most common malignant form of diseases in humans, particularly in the white population (D'Orazio et al., 2013; Rogers et al., 2010). Skin cancer is broadly classified into two types based on its origin: non-melanoma skin cancer (NMSC) and melanoma.

Basal cell carcinoma (BCC) and squamous cell carcinoma (SCC) are classified as NMSCs. BCC and SCC develop in the basal and squamous (spinosum) layers of the epidermis respectively (Wood and Bladon, 1985). UV radiation is the primary cause of NMSC. UV-B is the most carcinogenic radiation and induces a tan in the skin. Long term exposure to UV-B results in photo-aging and cancer (Madan, 2009;

**Abbreviations:** EO, essential oil;  $\beta$ -C,  $\beta$ -caryophyllene; AO-(2), aromadendrene oxide 2; P, phytol;  $\beta$ -caryophyllene/aromadendrene oxide 2, ( $\beta$ -C/AO-(2));  $\beta$ -caryophyllene/phytol, ( $\beta$ -C/P); Aromadendrene oxide 2/phytol, (AO-(2)/P); MTT, 3-(4,5-dimethyl thiazol-2-yl)-2,5 diphenyl tetrazolium bromide; AO, acridine orange; EtBr, ethidium bromide; PI, propidium Iodide; MMP, mitochondrial membrane potential ( $\Delta\Psi_m$ ); JC-1, 5,5',6,6'-tetrachloro-1,1',3,3' tetra ethyl benzimidazolyl carbocyanine iodide; DCFH-DA, 2,7- dichlorofluorescein diacetate; ROS, reactive oxygen species; NAC, N-acetyl cysteine; 5-FU, 5-Fluorouracil; Fa, fraction affected; CI, combination index; DRI, dose reduction index; and S, supplementary

\* Corresponding author.

E-mail address: [vermars@iitm.ac.in](mailto:vermars@iitm.ac.in) (R.S. Verma).<https://doi.org/10.1016/j.phymed.2018.05.001>

Received 31 December 2017; Received in revised form 24 March 2018; Accepted 1 May 2018

0944-7113/ © 2018 Elsevier GmbH. All rights reserved.

Maddodi and Setaluri, 2008). Exposure to UV radiation produces specific mutations in keratinocytes which leads to precancerous stage of actinic keratosis and development of skin cancer (Ortonne, 2002; Rodust et al., 2009). Local treatment of NMSC is determined based on the type, size, location of the lesion and patient age. Radiotherapy and surgery are the main treatment strategies (McGuire et al., 2009).

Natural products such as essential oils from aromatic plants are currently used in cancer prevention and therapeutic strategies. There have been studies showing the interactions among EO components, viz., antibacterial effects of *Cymbopogon citratus* where the major active components, geranial ( $\alpha$ -citral) and neral ( $\beta$ -citral) are potentiated by a non-active minor component, myrcene (Onawunmi et al., 1984). Low et al studied the synergism of the major components of *Eucalyptus citriodora* (where the major components citronellal and citronellol exhibited a 4-fold potentiation when combined in their naturally occurring ratio (90:7.5, respectively) compared to each component tested on its own (Low et al., 1974). In recent years comparative studies on the whole crude essential oil and its major compound from *Cymbopogon flexuosus* (Kumar et al., 2008), *Monarda citriodora* (Pathania et al., 2013) and *Piper cernuum* (Girola et al., 2015) have been studied for their anticancer activities. Our previous study (Pavithra et al., 2017) has demonstrated apoptotic activity of EO from *P. missionis* in A431 skin cancer and precancerous HaCaT cells wherein GC–MS analysis revealed the presence of  $\beta$ -caryophyllene (25.40%), as the major component, along with 4(14),11-eudesmadiene (7.17%), aromadendrene oxide 2 (14.01%) and phytol (6.88%). The present study investigates the role, interactions among EO components of *P. missionis* and underlying mechanism for induction of apoptosis in A431 skin epidermoid carcinoma and HaCaT cells (representing an early stage of skin cancer keratosis).

## Materials and methods

### Chemicals and antibodies

EO components of *P. missionis*  $\beta$ -caryophyllene, aromadendrene oxide 2 and phytol > 98% purity were obtained from Sigma-Aldrich (St. Louis, MO, USA). Stock solutions (100 mM) of these compounds were made in absolute ethanol. Stock solutions were further diluted to make a working stock solution of 1 mM, which was diluted to desired final concentrations with growth medium just before use. MTT 3-(4,5-dimethyl thiazol-2-yl)-2,5 diphenyl tetrazolium bromide (SRL), Propidium Iodide, 2,7-dichlorofluorescein diacetate, N-acetyl cysteine and  $\beta$ -Actin antibody were purchased from Sigma–Aldrich. Annexin V-FITC/PI kit and JC-1 dye were procured from Abcam (Cambridge, U.K.) and RNase A from MP Biomedical (Santa Ana, California, USA). Anti caspase-3 (cleaved) (Cat. No 9665) and anti caspase-9 (cleaved) (Cat. No 7237) were obtained from Cell Signaling Technology (Danvers, Massachusetts, USA), anti caspase-8 (cleaved) (Cat. No sc-6136) from Santa Cruz Biotechnology (Dallas, Texas, USA) and anti-Bax (Cat. No 04–434) from Millipore (Burlington, Massachusetts, United States). Anti-Cytochrome c (Cat. No ab90529), anti-Bcl2 (Cat. No ab7973) and anti-PARP (Cat. No ab32138) were procured from Abcam (U.K.). Anti-Cyclin D (Cat. No BD 556,470) antibody was procured from BD Biosciences (San Jose, CA, USA).

### Cell culture

A431 human epidermoid skin cancer cell line and HaCaT cell line for the study were obtained from National Centre for Cell Science, Pune, India. Cell lines were grown and maintained in RPMI-1640 medium supplemented with 10% heat-inactivated fetal bovine serum, L-glutamine (200 mM), 100 U/ml penicillin and 100Ug/ml streptomycin. The cells were incubated at 37 °C in a 5% CO<sub>2</sub> incubator. Human Mesenchymal stem cells (isolated from umbilical cord) were cultured in alpha MEM medium supplemented with 10% heat-inactivated fetal bovine serum (FBS), L-glutamine (200 mM), 100 U/ml penicillin and

100Ug/ml streptomycin. All the cells were maintained in a humidified 5% CO<sub>2</sub> incubator at 37 °C.

### MTT assay

Cytotoxicity of EO components on A431 and HaCaT cell lines were assessed by the MTT assay (Mosmann, 1983). In this study essential oil components:  $\beta$ -caryophyllene, aromadendrene oxide 2 and phytol individually were tested for cytotoxic activity on A431 and HaCaT cells at increasing concentrations for 72 h. 5-FU was used as positive control. Briefly, cells at exponential growth phase were taken up for the study. 5000 cells per well were seeded in 96-well plate. After overnight incubation, media was removed and cells were incubated with fresh medium containing increasing concentrations (10 to 200  $\mu$ M) of  $\beta$ -caryophyllene, AO-(2) and phytol for 72 h respectively. After the incubation period 10  $\mu$ l of MTT (5 mg/ml) was added to cells and plates were incubated at 37 °C for 3 h. The MTT-formazon product formed was dissolved in quenching solution (20% SDS in 50% dimethylformamide). Absorbance was measured at 570 nm (with reference at 620 nm) in an ELISA plate reader. The percent of cell viability was determined by dividing the absorbance of the treated cells with the corresponding absorbance of control (untreated cells). Experiments were repeated three independent times.

### Analysis of interaction among components

The interactions among the components  $\beta$ -caryophyllene, AO-(2) and phytol for cytotoxic activity were assessed by Isobolographic analysis (Chou and Talalay, 1984; Tallarida, 2006) and Combination Index (CI) method (Chou and Talalay, 1983, 1984). Three different combinations, i.e.,  $\beta$ -caryophyllene/aromadendrene oxide 2 ( $\beta$ -C/ AO-(2)),  $\beta$ -caryophyllene/phytol ( $\beta$ -C/P) and aromadendrene oxide 2/phytol (AO-(2)/P) were constituted for analysing the interactions. For combination studies, ratio of the two components was set from the IC<sub>50</sub> values of the single components. The IC<sub>50</sub> values were subjected to 2, 4, 8, 16 and 32 fold reduction and five concentration pairs were made for each combination. Cytotoxic effects of three combinations pairs were determined on A431 and HaCaT cells for 24, 48 and 72 h by MTT assay as described previously. The CI method was used to detect the type of pharmacological interaction among the components in the combinations (viz.,  $\beta$ -C/ AO-(2),  $\beta$ -C/ P and AO-(2)/P). The CI for the combinations were calculated using Chou and Talalay method:

$$CI = \frac{(D)_1}{(Dx)_1} + \frac{(D)_2}{(Dx)_2}$$

where (D)<sub>1</sub> and (D)<sub>2</sub> are the individual concentrations of the two components in combination which gives x% effect. (Dx)<sub>1</sub> and (Dx)<sub>2</sub> are the concentrations of the single components alone that gives the same x % effect (isoeffective) (i.e., 50% growth inhibition in our study). Experiments were repeated thrice independently. Interaction among components of the combinations were determined by Fa-CI plot using the CompuSyn software (Chou and Martin, 2005) (Paramus, NJ, USA). The value of CI = 1 indicates an additive effect between the two components, whereas a CI < 1 or > 1 indicates synergism or antagonism respectively. The dose-reduction index (DRI) defines how many folds the dose of each drug in a combination is reduced at a given effect level when compared with the doses of each drug alone (Chou TC 1998) i.e.,

$$(DRI)_1 = (Dx)_1/(D)_1$$

$$(DRI)_2 = (Dx)_2/(D)_2$$

The DRI > 1 indicates the reduced dose for a given drug combination compared with the dose of that drug alone. DRI for the components in the three combinations were calculated.

### Detection of nuclear morphology changes by AO/EtBr staining

A431 and HaCaT cells undergoing morphological and nuclear changes upon treatment with EO component combinations were detected by AO/EtBr staining (Ribble et al., 2005). Approximately 5,000 cells were seeded in 96-well plate, allowed to attach for an overnight period and treated with the combinations of  $\beta$ -caryophyllene/AO-(2) ( $\beta$ -C 12.5  $\mu$ M, AO-(2) 6.25  $\mu$ M),  $\beta$ -caryophyllene/phytol ( $\beta$ -C 25  $\mu$ M, P 21.75  $\mu$ M), AO-(2)/ phytol (AO-(2) 25  $\mu$ M, P 43.5  $\mu$ M) for A431 cells respectively and  $\beta$ -caryophyllene/AO-(2) ( $\beta$ -C 12.5  $\mu$ M, AO-(2) 9.5  $\mu$ M),  $\beta$ -caryophyllene/phytol ( $\beta$ -C 25  $\mu$ M, P 17.5  $\mu$ M) and AO-(2)/phytol (AO-(2) 38  $\mu$ M, P 35  $\mu$ M) for HaCaT cells respectively for 72 h. After incubation period, cells were stained with 1  $\mu$ l of Acridine Orange (100  $\mu$ g/ml) and 1  $\mu$ l of EtBr (100  $\mu$ g/ml) dye (Sigma-Aldrich) and incubated in dark for of 15 min. Cells were visualized and photographed immediately using a fluorescence microscope (Eclipse Ti-E, Nikon, Melville, NY, U.S.A.).

### Cell cycle analysis

Cell cycle analysis was determined using flow cytometry. Briefly  $1 \times 10^5$  cells/ml exponentially growing cells were seeded in 6-well culture plates. The medium was replaced and cells were exposed to medium containing individual components  $\beta$ -caryophyllene, AO-(2), phytol and their combinations  $\beta$ -C/ AO-(2),  $\beta$ -C/P and AO-2/P for 72 h. After the incubation period, untreated and treated cells were collected from the treatment wells. Cells were washed with PBS and fixed in 70% “ice” cold ethanol overnight at 4°C. Fixed cells were centrifuged and washed in PBS to remove residual ethanol. The pellets were re-suspended in 300  $\mu$ l of PBS containing Propidium Iodide (PI) (50  $\mu$ g/ml), 0.5% Triton X and incubated with RNase A (50  $\mu$ g/ml) at 37 °C for 30 min in water bath (Darzynkiewicz and Juan, 1997). After staining, cells were analyzed on a FACS Calibur flow cytometry (BD Bioscience). Cells in G0/G1, S, G2/M and sub-G1 phases were detected. Data were analyzed using Flow Jo software.

### Detection of apoptosis by Annexin V FITC/PI assay

Induction of apoptosis by individual components  $\beta$ -caryophyllene, AO-(2), phytol and their combinations in A431 and HaCaT cells was determined by flow cytometry using Annexin V-FITC/PI staining assay kit (Abcam) according to manufacturer's protocols with slight modifications. A431 and HaCaT cells were treated with individual EO components and their combinations comprising  $\beta$ -caryophyllene/ AO-(2),  $\beta$ -caryophyllene/phytol and AO-(2)/phytol for 72 h. Cells were washed and suspended in 300  $\mu$ l binding buffer and stained with Annexin V/FITC (1.5  $\mu$ l) antibody and PI (1.5  $\mu$ l) and incubated in dark for 5 min. Stained cells were analyzed by Flow Cytometry using quadrant statistics to detect live, early apoptotic, late apoptotic and necrotic cell populations. Data were analyzed using Flow Jo software.

### Measurement of mitochondrial membrane potential

Loss of mitochondrial membrane potential was assessed using JC-1 dye. Briefly ( $1 \times 10^5$ /ml) cells were incubated with the combinations:  $\beta$ -C/ AO-(2),  $\beta$ -C/P and AO-2/P for 72 h. Then the cells were washed with PBS and incubated with complete medium containing JC-1 dye (10  $\mu$ M) at 37 °C for 30 min in dark. Cells were pelleted, re-suspended in PBS and analyzed by flow cytometry. Loss of MMP in treated cells was detected by the decrease in FL-2 fluorescence (red) and increase in FL-1 fluorescence (green).

### Measurement of intracellular ROS production

Intracellular ROS generation in cells was determined with H2DCF-DA. A431 and HaCaT cells were seeded in six-well plates at a density of

$1 \times 10^5$  cells/ml and allowed to adhere overnight. The medium was removed and cells were incubated with fresh medium containing individual components  $\beta$ -C, AO-(2), P and their combinations  $\beta$ -C/ AO-(2),  $\beta$ -C/ P and AO-(2)/P for 72 h. Treated cells were washed with PBS and incubated with H2DCF-DA (10 $\mu$ M) for 30 min in the dark, then analyzed immediately by flow cytometry (Ameziane-El-Hassani et al., 2010) and the Median Fluorescence Intensity (MFI) was recorded. Data acquisition ( $10^4$  events for each sample) was performed with Cell Quest software.

### Western blot analysis

To detect the presence of apoptosis related proteins, A431 and HaCaT cells were subjected to treatment with combinations comprising  $\beta$ -C /AO-(2),  $\beta$ -C/P and AO-(2)/P for a period of 72 h. Treated and untreated cells were collected by trypsinisation and cell pellets were re-suspended in RIPA cell lysis buffer (10 mM Tris Hcl, pH8.0, 1 mM EDTA, 1% Triton X, 0.1% sodium deoxycholate, 0.1% Sodium dodecyl Sulphate, 140 mM sodium chloride) along with Protease inhibitor cocktail (Sigma) and incubated at 4 °C for 30 min. Cell lysates were then subjected to centrifugation at 10,000 x g for 10 min and the supernatant was transferred into a new tube. Cytosolic fractions of treated cells were prepared following the protocol of cytoplasmic extraction kit (Thermo scientific). Protein content of the cell lysates were quantified using the Bradford method (Bradford, 1976) with BSA as standard. Equal amounts of protein (30  $\mu$ g/sample) were separated electrophoretically by 12% SDS-PAGE and blotted onto Nitrocellulose membranes. After transfer, membranes were stained with 0.5% Ponceau stain in 1% acetic acid to confirm transfer of protein on membrane. Non-specific binding sites were blocked by incubating the membrane in 5% dried skimmed milk in TBST solution at room temperature for 1 h. Membranes were then incubated overnight at 4 °C with primary antibodies: anti caspase-3 at (1:400), anti caspase-8 (1:1000), anti caspase-9 at (1:400), anti-Bax at (1:400), anti-Cytochrome c at (1:1000), anti-Bcl-2 at (1:400), anti-PARP at (1:1000), anti Cyclin D antibody at (1:1000) and anti  $\beta$  actin at (1:5000) dilution in 3% BSA was prepared in TBS-Tween solution respectively. Next blots were probed with specific HRP conjugated secondary antibodies (1:10,000) (Sigma Aldrich, USA) respectively for 1 h at room temperature. This was followed by three washes with Tris-buffered saline with 0.1% Tween 20 (Sigma Aldrich, USA) (TBST) buffer. Each wash was done for 10 min at room temperature with constant shaking. The specific protein bands were detected using an enhanced Chemiluminescence detection kit, Super signal pico (Pierce, USA). Chemiluminescence intensity was captured using ChemiDoc Imaging system (Bio-Rad, USA).

### Colony formation assay

A431 and HaCaT cells (1000 cells/well) were seeded in six-well plates, allowed attach and exposed to the three combinations:  $\beta$ -C/AO-(2),  $\beta$ -C/P and AO-(2) /P for 72 h. After incubation period the medium was replaced with fresh medium and surviving cells were allowed to grow and form colonies (colony containing 50 cells) for 14 days. Colonies were fixed in ice cold methanol and stained with 0.5% crystal violet stain. Excess stain was removed by washing plates in water, air dried and photographed (Franken et al., 2006). Stained colonies in the control and treated cells were counted by using Image J software. Percentage colonies formed were calculated as: [(number of colonies formed by treated cells)/(number of colonies formed by untreated cells)] x100. Experiments were repeated three independent times.

### Tumor spheroids

Multicellular Tumor spheroids were generated as described previously (Ho et al., 2012) with slight modifications as described below. Spheroids were produced by seeding cells in 96 well plates coated with

2% w/v agar. Briefly, A431 cells at density of 25,000/well and HaCaT cells at density of 50,000/well were seeded in 200  $\mu$ l of RPMI media containing 10% FBS in 96 well plates. Cells were allowed to aggregate and form spheres for period of 48 h. In this study multicellular tumor spheroids of A431 and HaCaT cells of size (350–400  $\mu$ m) were generated and exposed to fresh media containing increasing concentrations of combinations  $\beta$ -C/AO-(2),  $\beta$ -C/P and AO-(2)/P (based on their  $IC_{50}$  values of individual components deduced for spheroid viability) for 72 and 96 h at 37 °C in a 5%  $CO_2$  incubator. Cell viability was determined by MTT assay. Spheroid size reduction upon treatment was measured using Nikon Ti pad software.

### Statistical analysis

Results are presented as the mean  $\pm$  SD. Statistical analysis of data was performed using a two-tail student *t*-test and one-way analysis of variance (ANOVA) with the Bonferroni multiple comparisons test using Graph Pad Prism Software. *p* value < 0.05 were considered statistically significant.

## Results

### Combinatorial interaction studies

$\beta$ -caryophyllene, aromadendrene oxide 2 and phytol exhibited a significant concentration-dependent cytotoxic effect by reducing cell viability of A431 and HaCaT cells at 72 h (S Fig. 1A and B). The  $IC_{50}$  values for above components in the order are 100  $\mu$ M, 50  $\mu$ M and 87  $\mu$ M respectively for A431 and 100  $\mu$ M, 76  $\mu$ M and 70  $\mu$ M respectively for HaCaT cells (Table 1). In order to determine the interactions among the components of EO from *P. missionis* for their cytotoxic effect in A431 and HaCaT cells, three pairs, viz.,  $\beta$ -C/AO-(2),  $\beta$ -C/P and AO-(2)/P were studied. Using the  $IC_{50}$  values of single components, five concentration pairs (of fixed ratio) for each combination were selected and their cytotoxic activity on A431 and HaCaT cells were determined. The results of MTT assays showed that  $\beta$ -C/AO-(2),  $\beta$ -C/P and AO-(2)/P combinations reduced the viability of A431 and HaCaT cells in a concentration and time dependent manner (Fig. 1A, B and C). The concentration of components in the combinations and their ratios that caused 50% reduction in viability of A431 and HaCaT cells are shown in Table 1. Combination of  $\beta$ -C/AO-(2),  $\beta$ -C/P and AO-(2)/P did not exhibit cytotoxic effects on HMSCs at 72 h (Supplementary Fig. 2).

Isobologram and combination index method was used to ascertain the nature of interaction among the components. The type of interactions among component pairs, i.e.,  $\beta$ -C/AO-(2),  $\beta$ -C/P and AO-(2)/P was assessed by isobologram method and the results are illustrated in Fig. 2. Isobologram was constructed for the combinations of  $\beta$ -C/AO-(2),  $\beta$ -C/P and AO-(2)/P using the respective  $IC_{50}$  values of the components,  $\beta$ -caryophyllene, AO-(2) and phytol obtained from cytotoxicity studies (S Fig. 1). Line of additivity was obtained by connecting the  $IC_{50}$  values of single components alone that caused 50% reduction in cell viability. The experimentally derived dose-pair combination that also caused 50% reduction in cell viability was plotted in the isobologram. The combination dose-pair point occurring on the lower left side of line of additivity indicates synergism, while that on upper right side of line of additivity indicates antagonism and the combination dose pair point on the line of additivity indicates an additive effect (Chou, 2006). Interestingly, in this study two types of interactions among the components in induction of cytotoxicity on A431 and HaCaT cells was observed. Analysis of the interactions revealed experimental  $IC_{50}$  value occurred on lower left side of the additive line, indicating synergistic interaction between  $\beta$ -C and AO-(2) as well as for the second combination i.e.,  $\beta$ -C and P in A431 and HaCaT cells (Fig. 2A and B). An additive effect was observed for AO-(2) and P as the experimental  $IC_{50}$  value occurred on the line of additivity for A431 and HaCaT cells (Fig. 2A and B).

The combination index (CI) analysis revealed a CI values < 1 for  $\beta$ -C/AO-(2) and  $\beta$ -C/P combinations indicating synergism, while for AO-(2)/P combination, the value of CI = 1 indicated an additive effect. Further, the Fa-CI plot i.e., fraction affected Fa (50% in our study) versus combination index showed synergistic (CI < 1) cytotoxic effect for combinations of  $\beta$ -C/AO-(2) and  $\beta$ -C/P while an additive effect for AO-(2)/P combination (Fig. 2C). Details of CI values for A431 and HaCaT cells are shown in Table 2. Combinations  $\beta$ -C/AO-(2),  $\beta$ -C/P and AO-(2)/P exhibited 8 to 2 fold dose reduction for the components in the three combinations (Table 3). The concentrations of components in combinations (Table 1) are used in subsequent experiments to investigate the role as well as mechanism of synergistic interaction and additive effect in inducing apoptosis in A431 and HaCaT cells.

### Combination of components alter nuclear morphology

To know whether the cytotoxic effect induced by  $\beta$ -C/AO-(2),  $\beta$ -C/P and AO-(2)/P combinations on A431 and HaCaT cells was due to apoptosis, AO/EtBr staining by fluorescence microscopy was performed. Fig. 3 shows the nuclear morphology changes induced by  $\beta$ -C/AO-(2),  $\beta$ -C/P and AO-(2)/P combinations in A431 and HaCaT cells. Untreated cells had large nucleus and stained green. Treated cells exhibited apoptotic characteristics such as cell shrinkage, blebbing, condensed chromatin and stained green. The presence of apoptotic features in the treated cells confirms that the combinations of the components induce apoptosis in A431 and HaCaT cells.

### Effect of combination of components on cell cycle progression

To investigate the mechanism involved in the growth inhibitory effects of the combinations, viz.,  $\beta$ -C/AO-(2),  $\beta$ -C/P and AO-(2)/P in A431 and HaCaT cells, cell cycle analysis was performed. Fig. 4A reveal that when cells were treated with 12.5  $\mu$ M of  $\beta$ -caryophyllene alone for 72 h, an increase in the sub-G1 content of 12.3% compared to the control was seen. However, the cell cycle distribution did not show significant changes when treated with 6.25  $\mu$ M of AO-(2) alone for 72 h. Interestingly, A431 cells treated with the combination of  $\beta$ -C/AO-(2) ( $\beta$ -C 12.5  $\mu$ M and AO-(2) 6.25  $\mu$ M) showed remarkable increase in the sub-G1 content to 66% with loss of cells from G0/G1, S, G2/M phases (Fig. 4A). In HaCaT cells, individual treatments with  $\beta$ -C and AO-(2) alone did not show changes in the cell cycle distribution at 72 h. However, the treatment of HaCaT cells with  $\beta$ -C/AO-(2) combination ( $\beta$ -C 12.5  $\mu$ M and AO-(2) 9.5  $\mu$ M) caused significant increase in G0/G1 content to 73% (with loss of cells from S and G2/M phases) compared to G0/G1 content (53%) of untreated control cells (Fig. 4A).

The effect of combination of  $\beta$ -C/P on cell cycle progression of A431 and HaCaT at 72 h is shown in Fig. 4B. Percentage of apoptosis induced by  $\beta$ -C and P individually in A431 cells was 18.5% and 13% respectively as indicated by the sub-G1 peak. The percentage of cell in sub-G1 phase increased upon treatment with  $\beta$ -C/P combination ( $\beta$ -C 25  $\mu$ M and P 21.75  $\mu$ M) significantly to 45% at 72 h with loss of cells from G0/G1 phase (Fig. 4B). In HaCaT cells at 72 h, G0/G1 content for  $\beta$ -C treated cells was 53% and 57% for phytol treated cells. This combination ( $\beta$ -C 25  $\mu$ M and P 17.5  $\mu$ M) caused an increase in G0/G1 phase to 81% with loss of cells from S and G2/M phases when compared to control cells (G0/G1 content being 53%) causing cell cycle arrest (Fig. 4B). These results suggest that  $\beta$ -C/P combination inhibited growth of A431 and HaCaT cells by inducing apoptosis and cell cycle arrest at the G0/G1 phase.

Effect of third combination AO-(2)/P on A431 and HaCaT cells is shown in the Fig. 4C. The individual treatment with AO-(2) at 25  $\mu$ M alone resulted in 73% G0/G1 arrest and phytol treatment at 43.5  $\mu$ M increased the sub-G1 content to 15.5%. AO-(2)/P combination treatment (AO-(2) 25  $\mu$ M and P 43.5  $\mu$ M) increased the sub-G1 population to 47% with loss of cells from G0/G1 phase in A431 cells (Fig. 4C). In HaCaT cells individual treatment with AO-(2) at 38  $\mu$ M alone resulted

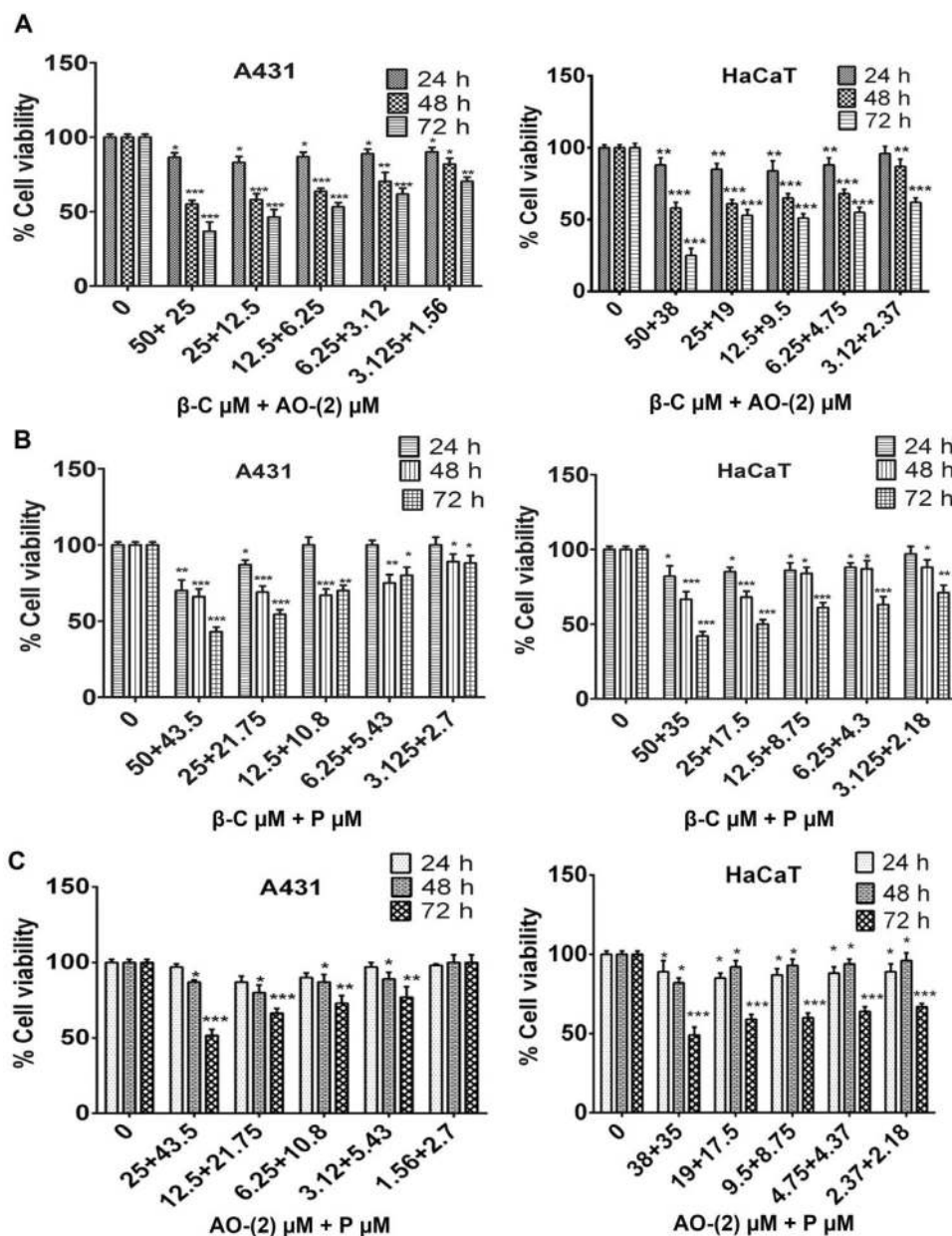


**Fig. 1.** Cytotoxic effects of the combination pair comprising components,  $\beta$ -caryophyllene ( $\beta$ -C), aromadendrene oxide 2 (AO-(2)) and phytol (P) on A431 and HaCaT cells. (A)  $\beta$ -C/AO-(2), (B)  $\beta$ -C/P and (C) AO-(2)/P. Cells were treated with increasing concentrations of the combinations for time period of 24, 48 and 72 h. Cell viability was determined by MTT assay. Data points represent the mean  $\pm$  SD of three individual experiments. Statistical significance is denoted by \* for  $p < 0.05$ , \*\*  $p < 0.01$  and \*\*\*  $p < 0.001$  compared with untreated control cells.

**Table 1**  
IC<sub>50</sub> values of single components and combination pairs for A431 and HaCaT cells.

Cell lines	Fixed ratio and concentration of components for the combination								
	$\beta$ -C	AO-(2)	P	$\beta$ -C/AO-(2)		$\beta$ -C/P		AO-(2)/P	
	IC <sub>50</sub> ( $\mu$ M)			Fixed ratio	( $\mu$ M)	Fixed ratio	( $\mu$ M)	Fixed ratio	( $\mu$ M)
A431	100	50	87	2:1	12.5/6.25	1.15:1	25/21.75	0.58:1	25/43.5
HaCaT	100	76	70	13:1	12.5/9.5	1.42:1	25/17.5	1.08:1	38/35

$\beta$ -C/AO-(2): $\beta$ -caryophyllene and aromadendrene oxide 2  
 $\beta$ -C/P: $\beta$ -caryophyllene and phytol  
 AO-(2)/P:aromadendrene oxide 2 and phytol  
 The fixed ratio for each combination is based on the IC<sub>50</sub> values of single components

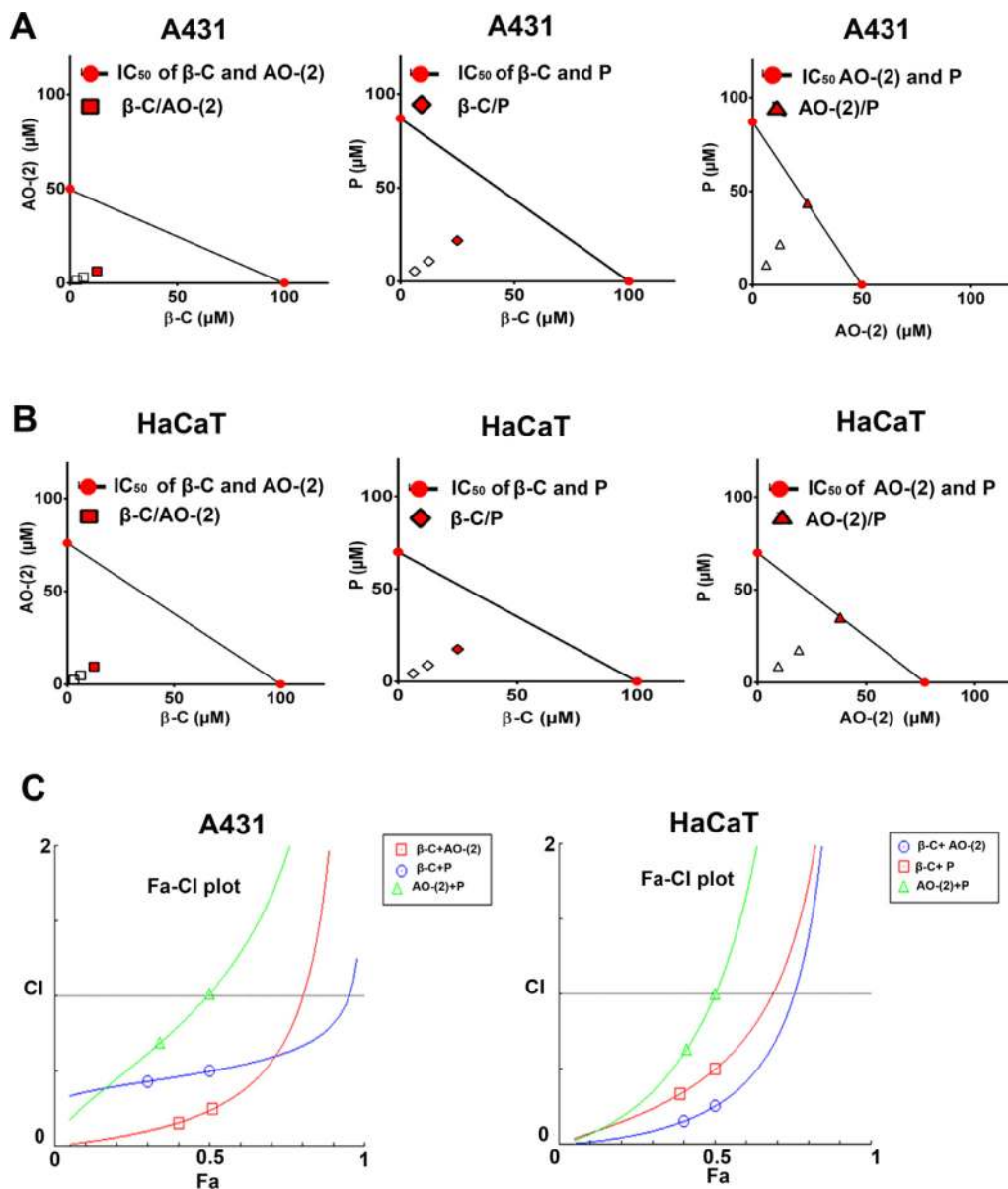


**Fig. 2.** Analysis of interactions among the components of combinations in exerting cytotoxic activity in A431 and HaCaT cells. (A and B) Isobologram showing dose-pair of components in the combination of β-caryophyllene (β-C)/aromadendrene oxide 2 (AO-(2)), β-caryophyllene (β-C)/phytol (P) and aromadendrene oxide 2 (AO-(2))/phytol (P) exhibiting 50% growth inhibition on A431 and HaCaT cells. (●) indicates IC<sub>50</sub> value of the individual components. The symbols (■, ◆, ▲) represent dose-pair combination exhibiting 50% growth inhibition. The data points (□, ◇, △) refer to dose-pair (of same fixed ratio) with growth inhibition < 50%. (C) Fa-CI plot (Chou-Talalay plot) showing interactions among the components in combinations for cytotoxic activity on A431 and HaCaT cells, Fa = 0.5. Fa is the fraction of cells affected by combination treatment.

**Table 2**  
Analysis of interactions among components in the combinations by Combination Index (CI) Method.

Combinations	Concentration of components in the combination (μM)		CI values		CI range, interaction and grade (Chou,1991)
	A431	HaCaT	A431	HaCaT	
β-C/AO-(2)	12.5/ 6.25	12.5/9.5	0.28	0.25	0.1–0.3 CI < 1 Strong synergism (+ + + +)
β-C/P	25/ 21.75	25/17.5	0.5	0.5	0.3–0.7 CI < 1 Synergism (+ + +)
AO-(2)/P	25/43.5	38/35	1	1	0.90–1.10 CI = 1 Additivism (±)

β-C/AO-(2):β-caryophyllene and aromadendrene oxide 2  
 β-C/P:β-caryophyllene and phytol  
 AO-(2)/P:aromadendrene oxide 2 and phytol  
 Combination index is a measure of the degree of drug interaction. CI values for the combinations in present study were calculated using CompuSyn software.

**Table 3**  
Dose reduction index (DRI) for components in combination for cell death (50%).

Cell lines	DRI for components in combination					
	β-C/AO-(2)		β-C/P		AO-(2)/P	
	β-C	AO-(2)	β-C	P	AO-(2)	P
A431	8	8	4	4	2	2
HaCaT	8	7.9	4	4	2	2

β-C/AO-(2):β-caryophyllene and aromadendrene oxide 2  
 β-C/P:β-caryophyllene and phytol  
 AO-(2)/P:aromadendrene oxide 2 and phytol  
 DRI was calculated using CompuSyn software. DRI > 1 depicts favourable dose reduction.

in 63% G0/G1arrest and phytol treatment with 35 μM resulted in sub-G1 content of 17.5%. While the combination treatment (AO-(2) 38 μM and P 35 μM) increased the G0/G1 content to 77% with loss of cells from S and G2/M phases leading to G0/G1cell cycle arrest compared to G0/G1content (53%) of control cells (Fig. 4C). Combinations of

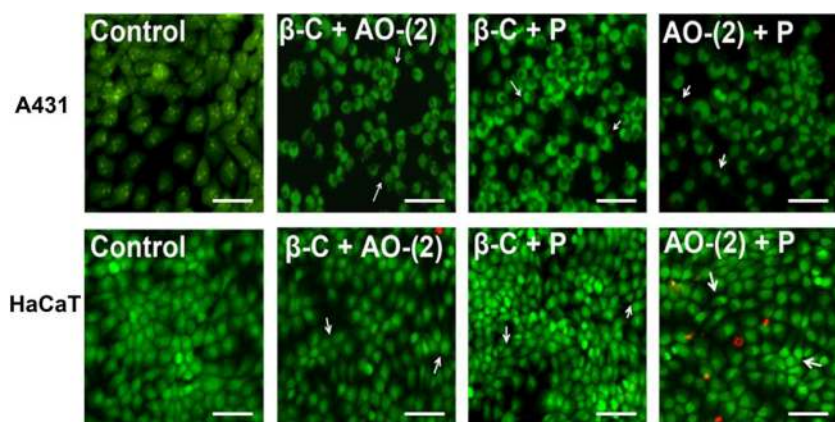


**Fig. 3.** Nuclear morphology changes induced by combination of components. Untreated and treated A431 and HaCaT cells with combinations of  $\beta$ -C + AO-(2),  $\beta$ -C + P and AO-(2) + P for 72 h. Cells were stained with AO/EtBr and viewed by fluorescence microscopy to detect the nuclear morphology changes undergone after the treatment. White Arrows indicate cells undergoing apoptosis. Scale bar: 100  $\mu$ m.

components inhibited the growth of A431 and HaCaT cells by increasing the sub-G1 content and causing cell cycle arrest at G0/G1 phase and accompanied by reduction in cyclin D protein levels (Fig 8D). These results conclude that the  $\beta$ -C/AO-(2),  $\beta$ -C/P and AO-(2)/P combinations were more effective than the individual treatments in exerting growth inhibitory effects.

#### Combination of components induce apoptosis

To further determine whether the observed cytotoxic activity caused by combinations of  $\beta$ -C/AO-(2),  $\beta$ -C/P and AO-(2)/P was through apoptosis or necrosis, Annexin-V FITC/PI staining assay by flow cytometry was performed. Dying cells are characterized as early apoptotic cells, in which the plasma membrane remains intact but exposes phosphatidylserine (PS) on the cell surface, while in late apoptotic cells the plasma membrane becomes permeabilized to dye Propidium Iodide. Apoptosis induced by  $\beta$ -C/AO-(2),  $\beta$ -C/P and AO-(2)/P combinations were confirmed by Annexin-V FITC/PI staining. As illustrated in Fig. 5, the results show that percentage of apoptotic cells in A431 and HaCaT cells by individual treatments with  $\beta$ -C and AO-(2) was not significant compared to the untreated cells. However, combination treatment with  $\beta$ -C/AO-(2) on A431 and HaCaT cells dramatically increased the apoptotic cell populations compared to the individual treatments (Fig. 5A). These results indicate that  $\beta$ -C/AO-(2) combination induced apoptosis in A431 and HaCaT cells.

The Fig. 5B shows the apoptosis effect induced by second combination  $\beta$ -C/P in A431 and HaCaT cells. The results obtained revealed that individual treatments with  $\beta$ -C and P alone induced apoptosis in A431 and HaCaT cells compared to untreated cells.  $\beta$ -C/P combination treatment further increased the apoptosis rates to 68.9% in A431 and 62% in HaCaT cells at 72 h. The apoptosis rates produced by the  $\beta$ -C/P combination ( $\beta$ -C 25  $\mu$ M and P 21.75  $\mu$ M) in A431 and ( $\beta$ -C 25  $\mu$ M and P 17.5  $\mu$ M) in HaCaT cells was significantly higher than the individual treatments. These results confirm that  $\beta$ -C/P combination induced apoptosis in A431 and HaCaT cells.

Effect of the third combination comprising AO-(2)/P is shown in the Fig. 5C. Results obtained revealed that AO-(2) and phytol individual treatments induced apoptosis in A431 and HaCaT cells compared to untreated cells. AO-(2)/P combination treatment increased the apoptosis rates to 75.2% in A431 and 87.3% in HaCaT cells at 72 h. The apoptosis rates produced by the AO-2/P combination (AO-(2) 25  $\mu$ M and P 43.5  $\mu$ M) in A431 and (AO-(2) 38  $\mu$ M and P 35  $\mu$ M) in HaCaT cells was significantly greater than the individual treatments. These results indicate that the  $\beta$ -C/AO-(2),  $\beta$ -C/P and AO-(2)/P combination treatments enhanced apoptotic cell death than the individual component treatments in A431 and HaCaT cells.

#### Combination of components causes loss of MMP ( $\Delta\Psi_m$ )

Changes in the mitochondrial membrane potential ( $\Delta\Psi_m$ ) have been originally correlated to be early events in the apoptotic signalling pathway. Loss of mitochondrial membrane potential triggered by combination of components in A431 and HaCaT cells were analysed by staining the cells with JC-1 a lipophilic cationic dye by flow cytometry. In healthy cells the JC-1 gets accumulated in the mitochondrial membrane as red aggregates (emits red fluorescence). JC-1 cannot accumulated in the collapsed mitochondrial membranes of apoptotic cells and hence appear as green monomers in the cytoplasm. The combination treatment caused loss of mitochondria membrane potential in A431 and HaCaT cells at 72 h (Fig. 6). In A431 cells,  $\beta$ -C/AO-(2),  $\beta$ -C/P and AO-(2)/P combinations led to loss of MMP in 57.3%, 51.6% and 40.7% of the cell population respectively, while in HaCaT cells 49.5%, 48.3% and 34.3% of cell populations exhibited loss of MMP respectively (Fig. 6). These results indicate that combination treatment caused mitochondrial damage with significant loss of  $\Delta\Psi_m$  in A431 and HaCaT cells.

#### Effect of combination of components on intracellular ROS

To investigate whether intracellular ROS was involved in apoptosis induced by the combinations  $\beta$ -C/AO-(2),  $\beta$ -C/P and AO-(2)/P in A431 and HaCaT cells, DCF fluorescence assay was performed by flow cytometry. Basal levels of ROS were detected in the control cells (untreated cells). Combination pair comprising  $\beta$ -C/AO-(2) in A431 and HaCaT cells increased ROS levels at 72 h. In A431 cells, individual treatment with  $\beta$ -C at 12.5  $\mu$ M raised ROS by 1.01 fold while AO-(2) at 6.25  $\mu$ M raised ROS level by 1.04 fold at 72 h. Surprisingly, their combination treatment for A431 at 72 h increased ROS by 1.63 fold compared to the untreated cells and individual treatments (Fig. 7A). In HaCaT cells, individual treatment with  $\beta$ -C at 12.5  $\mu$ M increased ROS by 1.04 fold while AO-(2) at 9.5  $\mu$ M increased ROS by 1.05 fold compared to control cells.  $\beta$ -C/AO-(2) combination treatment at 72 h caused 1.55 fold increase in ROS levels compared to untreated cells and individual treatment (Fig. 7A). Results from this study disclose that combination of  $\beta$ -C/AO-(2) induced intracellular ROS accumulation in A431 and HaCaT cells at 72 h.

The combination of  $\beta$ -C/P showed increase in ROS at 72 h. In A431 cells, individual treatment with  $\beta$ -caryophyllene at 25  $\mu$ M raised ROS by 1.03 fold while phytol at 21.75  $\mu$ M raised ROS level by 1.04 fold at 72 h. Remarkably,  $\beta$ -C/P combination treatment for A431 increased the ROS by 1.85 fold compared to the untreated cells and individual treatments (Fig. 7B). In HaCaT cells, individual treatment with  $\beta$ -caryophyllene at 25  $\mu$ M increased ROS by 1.08 fold while phytol at 17.5  $\mu$ M increased ROS by 1.01 fold compared to control cells.  $\beta$ -C/P combination treatment at 72 h caused 1.25 fold increase in ROS levels compared to untreated cells and individual treatment (Fig. 7B).

Also, the third combination of AO-(2)/P showed increase in ROS at

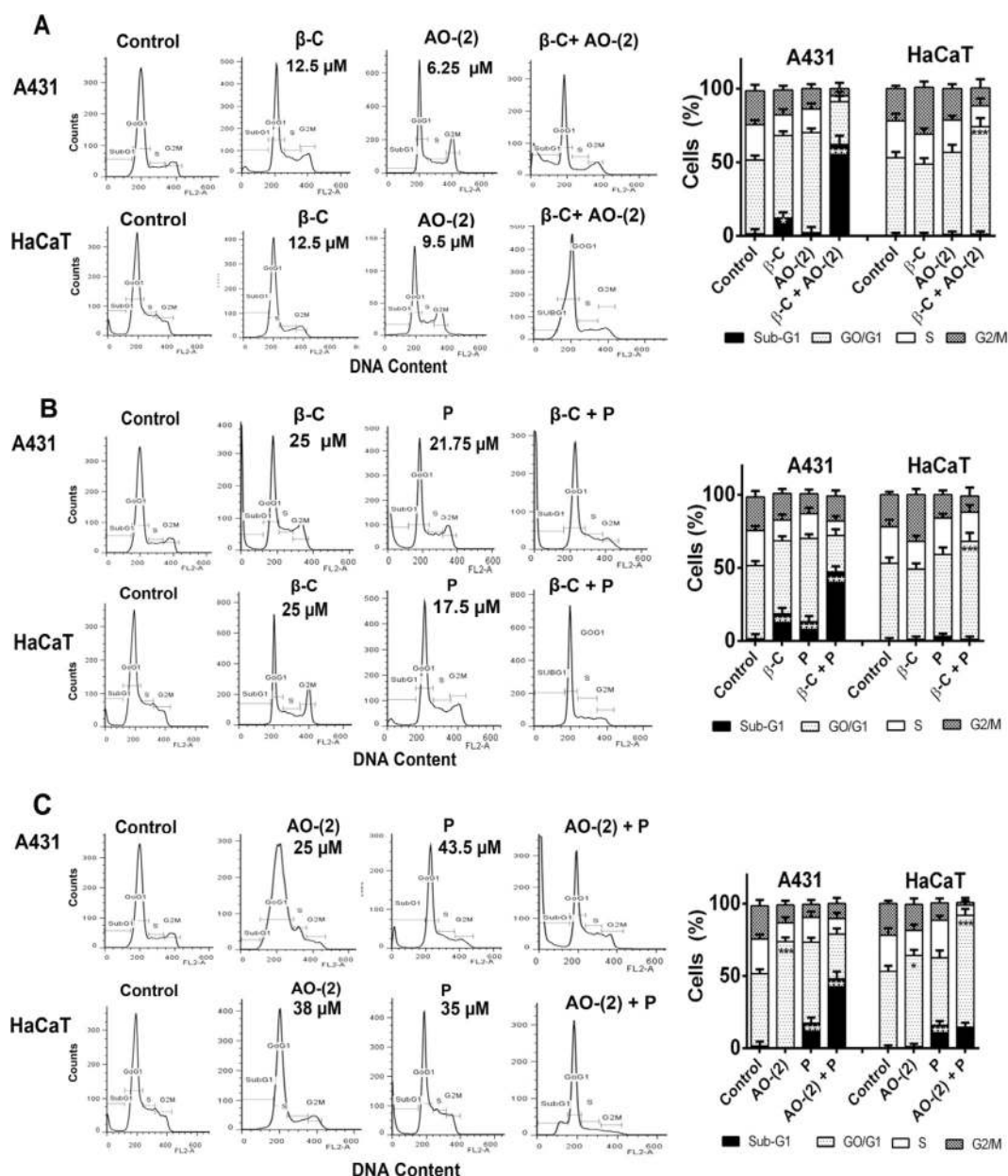


**Fig. 4.** Effect of individual components and combination treatment on cell cycle progression of A431 and HaCaT cells. (A)  $\beta$ -caryophyllene ( $\beta$ -C), aromadendrene oxide 2 (AO-(2)) alone and in combination (B)  $\beta$ -caryophyllene ( $\beta$ -C), phytol (P) alone and in combination and (C) aromadendrene oxide 2 (AO-(2)), phytol (P) alone and in combination. Right panels show percentage of cell population in Sub-G1, G0/G1, S and G2/M phases for untreated, individual and combination treatments. Data expressed as mean  $\pm$  SD of three independent experiments. The combination treatments were significant \*\*\*  $p < 0.001$  compared with untreated control cells, individual treatments.

72 h. In A431 cells, individual treatment with AO-(2) at 25  $\mu$ M and phytol at 43.5  $\mu$ M raised ROS by 1.10 and 1.08 fold. AO-(2)/P combination treatment increased the ROS by 1.7 fold compared to the untreated cells and individual treatments (Fig. 7C). In HaCaT cells, individual treatment with AO-(2) at 38  $\mu$ M and phytol at 35  $\mu$ M increased ROS by 1.16 and 1.05 fold compared to control cells. AO-(2)/P combination treatment caused 1.35 fold increase in ROS levels (Fig. 7C). These results reveal that treatment with the combinations, viz.,  $\beta$ -C/AO-(2),  $\beta$ -C/P and AO-(2)/P increased intracellular ROS accumulation compared to the individual component treatment in A431 and HaCaT cells.

*Measurement of ROS levels after pre-treatment with NAC*

In order to verify whether the apoptosis induced by the

combinations  $\beta$ -C/AO-(2),  $\beta$ -C/P and AO-(2)/P was due to ROS accumulation, A431 and HaCaT cells were pre-treated with NAC (250  $\mu$ M) for 2 h prior to treatment with combinations. At the end of treatment cell viability was determined by MTT assay. Cells were stained with Annexin V- FITC/PI and the percentage of apoptotic cells was determined by flow cytometry. Results revealed that pre-treatment of A431 and HaCaT cells with NAC cancelled apoptosis effects of  $\beta$ -C/AO-(2),  $\beta$ -C/P and AO-(2)/P combinations and increase in cell viability was observed (Fig. 7D, E, F and G). Results from this study confirm that  $\beta$ -C/AO-(2),  $\beta$ -C/P and AO-(2)/P combinations induced apoptosis through intracellular ROS accumulation in A431 and HaCaT.

*Effect of combination of components on apoptosis related proteins*

From the studies described above, it is noted the components in

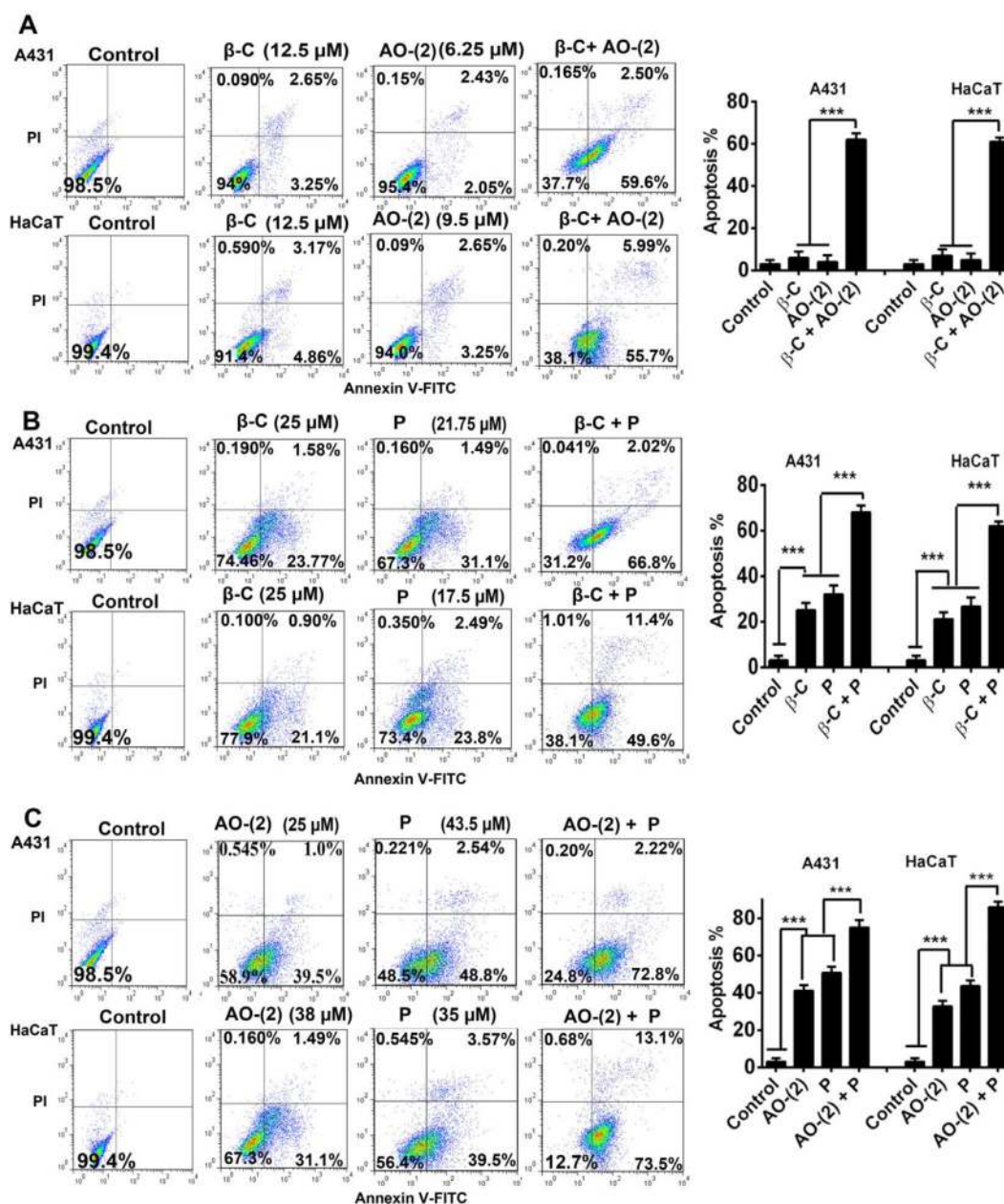


**Fig. 5.** Flow cytometry analysis for detection of apoptosis induced by individual components and their combination by Annexin V- FITC/PI staining on A431 and HaCaT cells. (A)  $\beta$ -caryophyllene ( $\beta$ -C), aromadendrene oxide 2 (AO-(2)) alone and in combination, (B)  $\beta$ -caryophyllene ( $\beta$ -C), phytol (P) alone and in combination, and (C) AO-(2), (P) alone and in combination. Right panels show apoptosis (%) in A431 and HaCaT cells treated with individual component and their combinations. Data expressed as mean  $\pm$  SD of three independent experiments. \*\*\*  $p < 0.001$  significant for individual component treatments compared with the control (untreated) cells, and also for combination treatment compared with individual component treatments. Quadrant analysis of gated cells were from 10,000 events. Cells in lower right represents early apoptosis (AV + /PI-) while cells in upper right quadrant represents late apoptosis (AV + /PI +) respectively.

combination shows better efficacy in terms of killing cells through synergistic and additive interactions than individually at specific concentrations. Hence, the role played by these combinations in reducing cell proliferation and ultimate cell death is studied. One of the processes of cell death is apoptosis. So we explored the expression of proteins related to apoptotic pathway upon treatment with combinations (Fig. 8). Western blot results revealed that treatment of A431 and HaCaT cells with  $\beta$ -C/AO-(2),  $\beta$ -C/P and AO-(2)/P combinations significantly decreased the expression of anti-apoptotic Bcl-2 protein level and increased Bax protein levels (Fig. 8A and B). Treatment of A431 and HaCaT cells with the combinations showed an increase in Bax/Bcl-2 ratios compared to untreated cells (Fig. 8C). Cytochrome c release was detected in the cytosolic fractions of treated A431 and HaCaT cells.

Treatment of cells with respective combination pairs for 72 h induced caspases activation and PARP cleavage. Cleaved forms of caspase-3 (17 kDa), caspase-8 (18 kDa), caspase-9 (37 kDa) and PARP cleavage (89 kDa) were detected in A431 and HaCaT cells treated with the combination of  $\beta$ -C/AO-(2),  $\beta$ -C/P and AO-(2)/P (Fig. 8A-B). HaCaT cells treated with  $\beta$ -C/AO-(2),  $\beta$ -C/P and AO-(2)/P combinations showed reduction in cyclin D protein levels (Fig. 8D).

*Combination of components inhibit colony formation*

The growth inhibitory activity of  $\beta$ -C/AO-(2),  $\beta$ -C/P and AO-(2)/P combinations by colony formation assay were studied. Colony formation assay is a cell survival assay based on the ability of single cells to

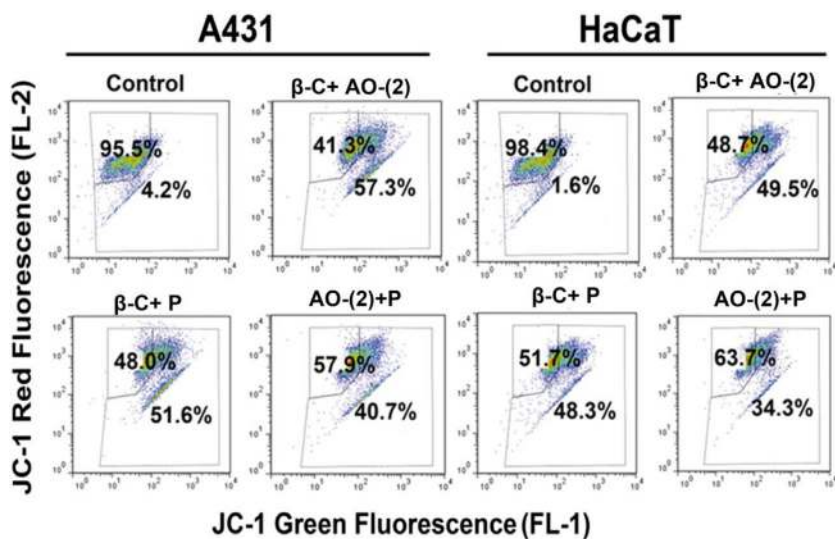


Fig. 6. The combination of components, β-caryophyllene (β-C) + aromadendrene oxide 2 (AO-(2)), β-caryophyllene (β-C) + phytol (P) and aromadendrene oxide 2 (AO-(2)) + phytol (P) induce loss of (ΔΨ<sub>m</sub>) MMP in A431 and HaCaT cells at 72 h. Cells were stained with JC-1 dye and analyzed by flow cytometry. Data displayed in Fig. are of mean of three similar experiments.

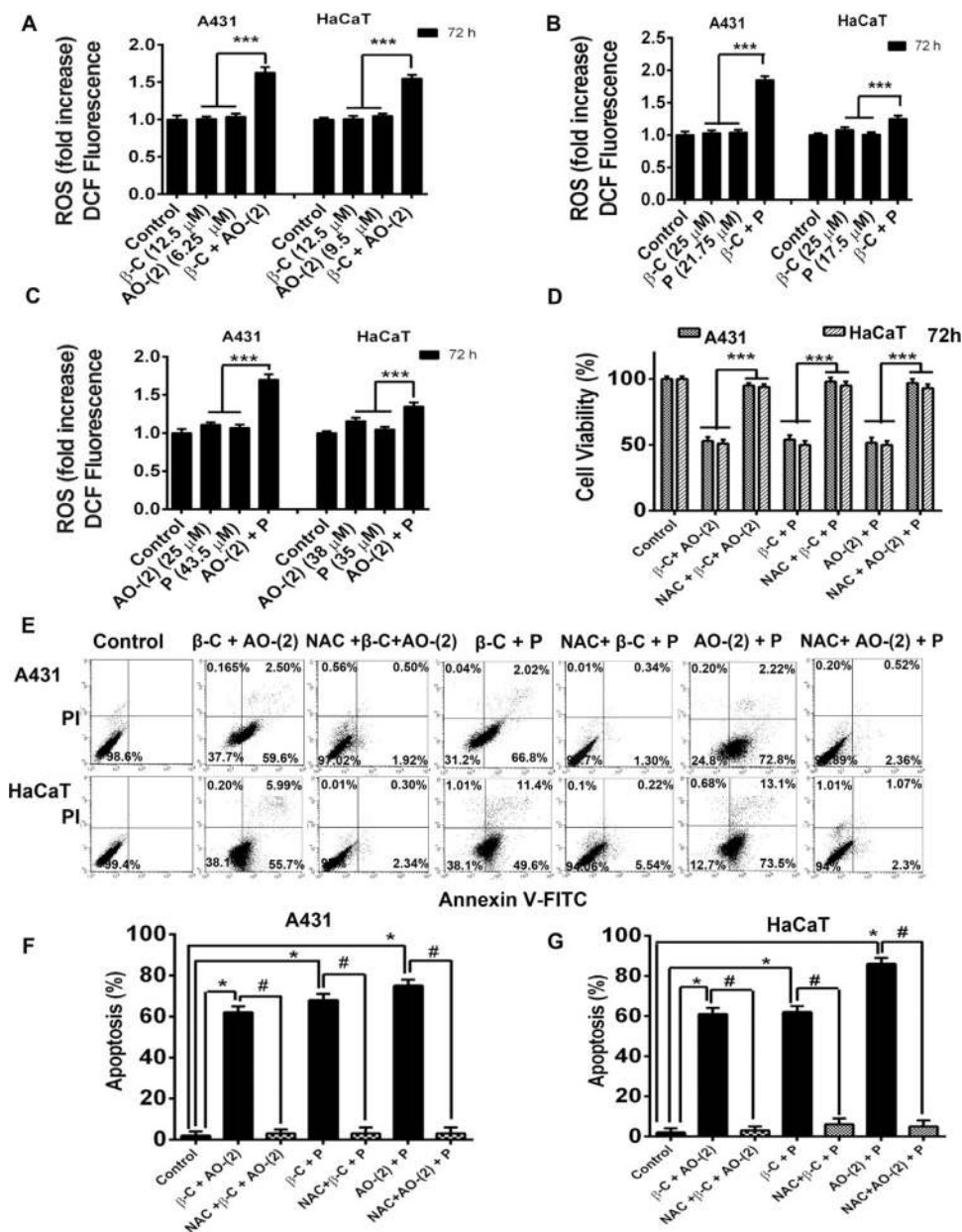
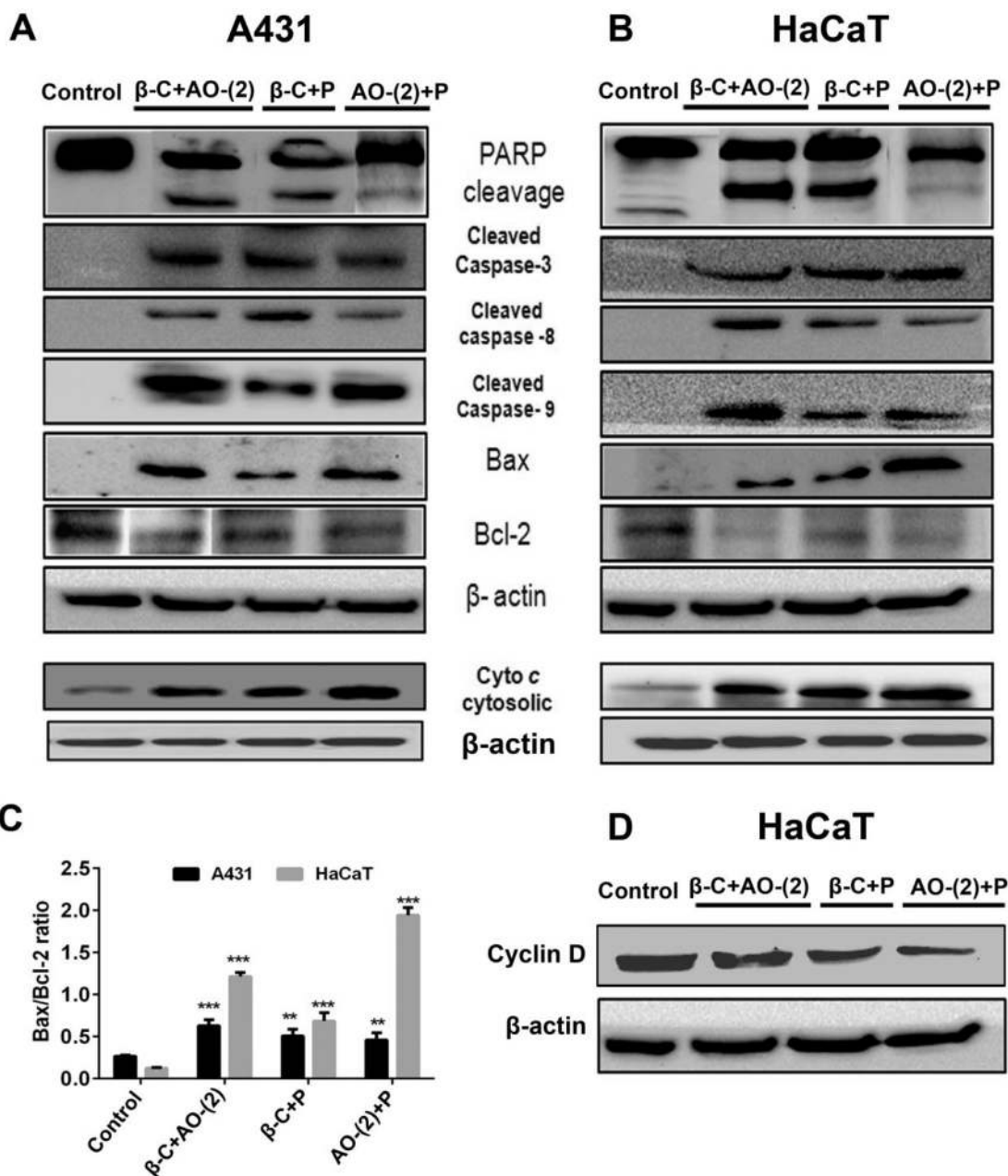


Fig. 7. Effect of individual component and their combination on intracellular ROS levels in A431 and HaCaT cells. (A) β-caryophyllene (β-C), aromadendrene oxide 2 (AO-(2)) alone and in combination (B) β-caryophyllene (β-C), phytol (P) alone and in combination and (C) AO-(2), P alone and in combination. Data represented is mean ± SD of three individual experiments. \*\*\*  $p < 0.001$  is significant compared to individual treatment groups. (D) Effect of NAC pre-treatment on viability of A431 and HaCaT cells at 72 h. Cell viability was measured by MTT assay. Data represent mean ± SD of three independent experiments. \*\*\*  $p < 0.001$ , significant difference between the designated groups viz., combination groups and NAC + combination groups. (E) Inhibition of apoptosis by NAC pre-treatment in A431 and HaCaT cells detected by Annexin V-FITC/PI staining. (F and G) Quantification of apoptotic cells without and with NAC treatment. Data represent mean ± SD of three independent experiments. Statistical significance is shown by \* (to indicate \*\*\*  $p < 0.001$ ) between the designated groups, i.e., untreated and combination treatment groups and # (points out \*\*\*  $p < 0.001$ ) between the two designated groups, viz., combination treatment and NAC + combination treatment.



**Fig. 8.** Effect of the combination of components on expression of apoptosis related proteins. (A) A431 cells treated with the combination of  $\beta$ -caryophyllene ( $\beta$ -C) + aromadendrene oxide 2 (AO-(2) (with 12.5  $\mu$ M + 6.25  $\mu$ M respectively),  $\beta$ -caryophyllene ( $\beta$ -C) + phytol (P) (25  $\mu$ M + 21.75  $\mu$ M) and aromadendrene oxide 2 (AO-(2) + phytol (P) (25  $\mu$ M + 43.5  $\mu$ M) for 72 h. (B) HaCaT cells treated with the combination of  $\beta$ -C + AO-(2) (with 12.5  $\mu$ M + 9.5  $\mu$ M respectively),  $\beta$ -C + P (25  $\mu$ M + 17.5  $\mu$ M) and AO-(2) + P (38  $\mu$ M + 35  $\mu$ M). (C) Effect of the combination of components on Bax/Bcl-2 ratios in A431 and HaCaT cells. \*\*  $p < 0.01$ , \*\*\* $p < 0.001$  compared with untreated control cells. (D) Effect of the combination of components on cyclin D protein levels in treated HaCaT cells for 72 h.  $\beta$ -actin was used as internal control.

grow into a colony after treatment with cytotoxic agents (Franken et al., 2006). Cells after treatment with  $\beta$ -C/AO-(2),  $\beta$ -C/P and AO-(2)/P were grown in fresh growth medium for 14 days and colonies formed were stained with crystal violet. The combinations of components inhibited the colony formation ability in the treated A431 and HaCaT cells (Fig. 9A). The percentage of colonies formed in A431 and HaCaT cells without and with the combination treatment (Fig. 9B). From the above data it is noted that in A431 cells,  $\beta$ -C/AO-(2),  $\beta$ -C/P and AO-(2)/P combinations inhibited colony formation by 79%, 74% and 73% respectively. The combination treatment in the order mentioned above resulted in 68%, 53% and 41% inhibition in colony formation for HaCaT cells. These results confirm that the combination treatment significantly inhibit the colony formation potential of A431 and HaCaT

cells.

#### Ex vivo toxicity study

In the present study 3D multicellular tumor spheroids (MCTs) of A431 and HaCaT cells were used for evaluating the growth inhibitory activity of combination of components. The spheroid models mimic the in vivo solid tumor in terms of micro environment and tumor organisation (Dufau et al., 2012). The combination treatment with  $\beta$ -C/AO-(2),  $\beta$ -C/P and AO-(2)/P caused reduction in viability of A431 and HaCaT cell spheroids at 96 h. IC<sub>50</sub> values for  $\beta$ -C/AO-(2),  $\beta$ -C/P and AO-(2)/P on A431 tumor spheroids were (65 $\mu$ M + 55  $\mu$ M), (100  $\mu$ M + 100  $\mu$ M) and (340  $\mu$ M + 400  $\mu$ M) respectively. Combination

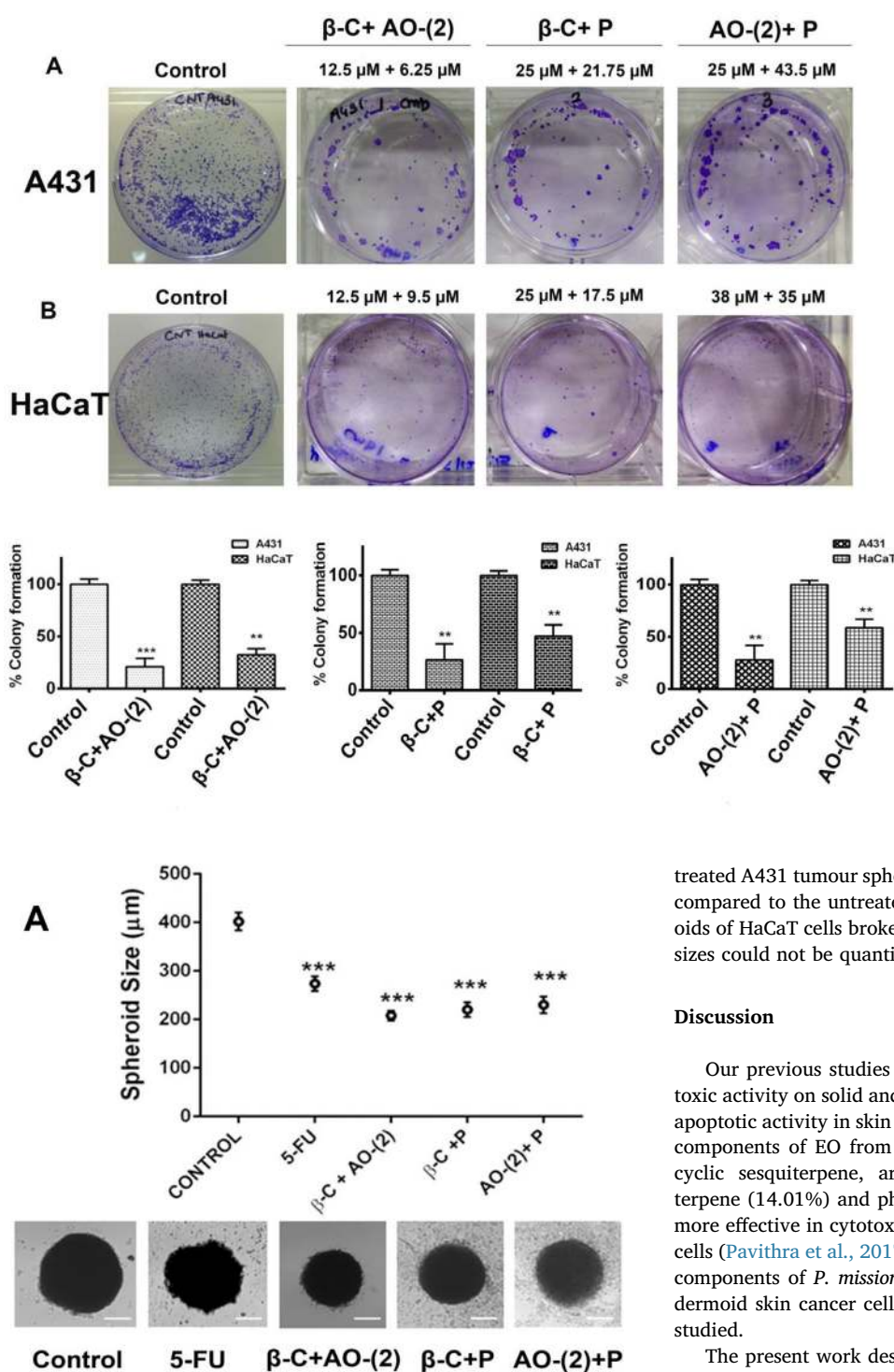


Fig. 9. Inhibitory effect of combination of components on colony formation of A431 and HaCaT cells. (A) Effect of the combination β-caryophyllene (β-C) + aromadendrene oxide 2 (AO-(2)), β-caryophyllene (β-C) + phytol (P) and AO-(2) + P on colony formation in A431 and HaCaT cells. (B) Percentage of colonies formed in A431 and HaCaT cells without and with the combination treatment. Data represented is mean ± SD of three independent experiments. \*\*  $p < 0.01$  and \*\*\*  $p < 0.001$ , compared to colonies formed in untreated control wells.

Fig. 10. Inhibitory effect of combination of components on growth of multicellular tumor spheroids. (A) Size reduction for A431 tumor spheroids after treatment with 5-FU and combination of components, β-caryophyllene (β-C) + aromadendrene oxide 2 (AO-(2)), β-caryophyllene (β-C) + phytol (P) and AO-(2) + P for 96 h. Scale bar: 100 μm. Data represented is mean ± SD of three independent experiments. \*\*\*  $p < 0.001$  compared with untreated control spheroids. Images shown are representative of one the three similar experiments.

treated A431 tumour spheroids (at  $IC_{50}$  value) exhibited size reduction compared to the untreated spheroids (Fig. 10A). As the treated spheroids of HaCaT cells broke down into fragments losing their shape, their sizes could not be quantified.

### Discussion

Our previous studies on crude EO from *P. missionis* revealed cytotoxic activity on solid and leukemic cancer cells and showed significant apoptotic activity in skin cancer cells. Study also showed that the major components of EO from *P. missionis* (β-caryophyllene (25.40%) a bicyclic sesquiterpene, aromadendrene oxide-(2) oxygenated sesquiterpene (14.01%) and phytol (6.88%) acyclic diterpene alcohol) were more effective in cytotoxic activity than crude EO on A431 and HaCaT cells (Pavithra et al., 2017). To delineate the mechanism exerted by the components of *P. missionis* EO on apoptosis in precancerous and epidermoid skin cancer cells, interaction among components of EO were studied.

The present work describes combinatory effect of β-caryophyllene, aromadendrene oxide 2 and phytol on growth inhibitory effects on skin epidermoid cancer cells. Previous studies have also demonstrated that β-caryophyllene significantly increased the anticancer activity of a-humulene, isocaryophyllene on MCF-7 cells and it potentiated the anticancer activity of paclitaxel (10 fold) in DLD-1 cell lines (Legault and Pichette, 2007). Yamaguchi and Levy (2016) demonstrated the interactive effects of β-caryophyllene with other botanical molecules. Their study showed that the combination of β-caryophyllene, baicalin and (+)-catechin exerted synergistic suppressive effects on the proliferation and synergistic stimulatory effects on the death of RAW267.4 cells in vitro. Suzuki et al. (1998) demonstrated the synergistic effect of the combination of phytol/retinol in the growth inhibition of mouse leukaemia L5178Y cells in-vitro.

The isobologram and combination index (CI) analysis revealed two

types of interactions to coexist among the component of *P. missionis* EO. Their possible mechanisms involved in growth inhibitory effects were analysed. The results demonstrate that the components  $\beta$ -C, AO-(2) and P exerted growth inhibitory and apoptotic activity through synergistic interactions in  $\beta$ -C/AO-(2) and  $\beta$ -C/P combinations and by additive effect in AO-(2)/P combination in A431 and HaCaT cells. This is attributed to increase Annexin positive cells, increase in sub-G1 content in case of A431 and G0/G1 arrest in HaCaT cells. The drug reduction index, DRI = 8 was noted for  $\beta$ -caryophyllene in combination with AO-(2) compared to  $\beta$ -caryophyllene alone.

In our study DCF-DA staining by flow cytometry showed significant ROS accumulation in A431 and HaCaT cells treated with the combinations than individual components. Inhibition of ROS by radical scavenger, NAC completely blocked the apoptosis induced by the combination treatments. Earlier studies have revealed that ROS induces apoptosis, DNA, protein and lipid damage in cancer cells (Lau et al., 2008). ROS can be cytotoxic when their levels reach a threshold that is no more compatible for cellular survival. This state may cause oxidative stress which hinder cancer cell progression (Fruehauf and Meyskens, 2007). The generation of ROS is reportedly involved in apoptosis induced by chemotherapeutic agents through the activation of the death receptor or mitochondria mediated apoptotic pathways (Moungjaroen et al., 2006; Prasad et al., 2010). Our findings confirm that apoptosis induced by combinations was through intracellular ROS accumulation.

Apoptosis is triggered through two signalling pathways: extrinsic mediated death receptor and intrinsic mediated by the mitochondrial initiated events (Elmore, 2007). Mitochondria play a central role in apoptosis. The BCL-2 family of proteins includes both pro-apoptotic (Bax, Bak) as well as anti-apoptotic molecules (BCL2, BCLxl). Indeed, the ratio between these two subsets helps determine, the susceptibility of cells to a death signal (Oltval et al., 1993). The disruption of the mitochondrial trans-membrane potential is an early event of the cell death process (Zamzami et al., 1995). Our study showed that treatment with  $\beta$ -C/AO-(2),  $\beta$ -C/P, AO-(2)/P combinations induced loss of the mitochondrial membrane potential, increase in Bax and decrease in Bcl-2 protein levels leading to increase in Bax/Bcl-2 ratios. Bax and Bak oligomers participate in forming pores and cause permeabilization of the outer mitochondrial membrane, leading to the release of the contents of the mitochondrial intermembrane space, including cytochrome *c* into the cytosol (Wang, 2001). These contents drive the activation of caspases, which are proteases that cleave and disable crucial proteins throughout the cell. Cytochrome *c*, initiates caspase activation when released from mitochondria during apoptosis (Liu et al., 1996). Combination treated A431 and HaCaT cells showed up regulation of cytochrome *c* in the cytosolic fraction. The release of cytochrome *c* from mitochondria to cytosol is essential for the formation of apoptosome and consequent activation of caspase-9 (Sun et al., 2004). Caspase-3, cysteine proteases plays a central role in the execution of the apoptotic program (Cohen, 1997) and is primarily responsible for the cleavage of PARP during cell death (Tewari et al., 1995). PARP is an enzyme involved in DNA repair, and its cleavage may inactivate their DNA repair system, which otherwise might impede progression of apoptosis (Patel et al., 1996). A characteristic event of apoptosis is the proteolytic cleavage of PARP. PARP cleavage is important marker for apoptosis induction (Lazebnik et al., 1994). In the present study combination treatments induced activation of caspases (caspases -3, -8 and -9) and cleavage of PARP in A431 and HaCaT cells. These results suggest that  $\beta$ -C/AO-(2),  $\beta$ -C/P, AO-(2)/P combinations induced cell death in A431 and HaCaT through activation of apoptotic pathway.

Mutations in the p53 gene have been detected in 50% of all human cancers and in almost all skin carcinomas (Basset-Seguain et al., 1994). It is well-known that p53 inactivation and mutant p53 expression provide cells with survival advantages, such as increased proliferation, evasion of apoptosis and chemo resistance (Brosh and Rotter, 2009). A431 cells carry a mutation at codon 273, resulting in a loss of trans-activating

activity (Park et al., 1994). HaCaT cells carry mutations at codons 179, 281 and 282, which are typical UV light-induced mutations (Lehman et al., 1993). It is interesting to observe from our findings that  $\beta$ -C/AO-(2),  $\beta$ -C/P, AO-(2)/P combinations were effective in killing A431 and HaCaT cells while the normal cells (HMSCs) remained unaffected upon treatment (Fig. S3). ROS-mediated cytotoxic processes that preferentially kill or inhibit tumor cell proliferation can be used as an effective strategy to target and eliminate cancer cells. This signifies the vital role of ROS as an aid in induction of apoptosis in p53-mutant A431 and HaCaT cells, which otherwise in other cancer models is generally routed via tumor suppressor gene like p53 or other oncogenes like Ras (Jasinski et al., 2008; Shukla et al., 2007).

Most of the time, the bioactivities of particular EO are decided by either one or two of its main components (Bakkali et al., 2008). But, sometimes overall activity cannot be attributed to any of the major constituents and the presence of a combination of molecules may exert significant effect. The experiments performed using concentration of 100/52/26  $\mu$ M respectively (close to natural proportions) of the three components ( $\beta$ -C/AO-(2)/P) resulted in 23% and 30% viability of A431 and HaCaT cells respectively (SFig. 3A and B). The combination of  $\beta$ -C/AO-(2)/P induced early and late apoptosis which was similar to that of crude EO (Pavithra et al., 2017) and the major component  $\beta$ -caryophyllene. The CI values calculated for the components  $\beta$ -C/AO-(2)/P (with Fa  $\sim$ 70% and IC<sub>70</sub> values deduced from cytotoxic study for individual components) showed that the overall interaction among the components in inducing apoptosis occurs through moderate synergism in A431 (CI = 0.74) and by additivism (near additive effect) in HaCaT cells (CI = 1.06). Also, SFig. 3 reveals that the components exhibit interdependency on each other and the activity of  $\beta$ -caryophyllene is accelerated by the presence of aromadendrene oxide 2 and phytol in inducing apoptosis in A431 and HaCaT cells.

## Conclusion

Our study revealed that combinations  $\beta$ -C/AO-(2) and  $\beta$ -C/P exhibited anticancer activity through synergistic interactions while AO-(2)/P via additive effect in A431 and HaCaT cells. The study shows that three combinations viz.,  $\beta$ -C/AO-(2),  $\beta$ -C/P and AO-(2)/P reduced cell viability, inhibited colony formation ability, induced cell cycle arrest and apoptosis in precancerous HaCaT cells and A431 human epidermoid skin cancer cells. The treatment of  $\beta$ -C/AO-(2),  $\beta$ -C/P and AO-(2)/P combination in A431 and HaCaT cells induced intracellular ROS accumulation, loss of mitochondrial membrane potential and alteration of several mediators at molecular level such as increase in Bax/Bcl-2 ratio, reduction in cyclin D levels, release of cytochrome *c*, activation of caspases (caspase-3, caspase-8, caspase-9) and cleavage of PARP. Results from our study suggest that combinations of  $\beta$ -caryophyllene with aromadendrene oxide 2 and phytol could be potential therapeutics for the treatment of precancerous and skin epidermoid cancer cells.

## Acknowledgment

This work was supported by the financial grant provided by the Department of Science and Technology (DST) New-Delhi, under the Women Scientist Scheme-A for the project SR/WOS-A/LS-260/2011 carried out at the Indian Institute of Technology Madras, Chennai-600036. The fellowship is offered to one of the authors, Pavithra P.S.

## Conflict of interest

The authors declare that there are no conflicts of interest to disclose.

## Supplementary materials

Supplementary material associated with this article can be found, in the online version, at doi:10.1016/j.phymed.2018.05.001.

## References

- Ameziane-El-Hassani, R., Boufraqueh, M., Lagente-Chevallier, O., Weyemi, U., Talbot, M., Métivier, D., Courtin, F., Bidart, J.-M., El Mzibri, M., Schlumberger, M., 2010. Role of H2O2 in RET/PTC1 chromosomal rearrangement produced by ionizing radiation in human thyroid cells. *Cancer Res.* 70, 4123–4132.
- Basset-Seguin, N., Moles, J.-P., Mils, V., Dereure, O., Guilhou, J.-J., 1994. TP53 tumor suppressor gene and skin carcinogenesis. *J. Invest. Dermatol.* 103.
- Brosh, R., Rotter, V., 2009. When mutants gain new powers: news from the mutant p53 field. *Nat. Rev. Cancer* 9, 701–713.
- Chou, T.-C., 2006. Theoretical basis, experimental design, and computerized simulation of synergism and antagonism in drug combination studies. *Pharmacol. Rev.* 58, 621–681.
- Chou, T.-C., Talalay, P., 1983. Analysis of combined drug effects: a new look at a very old problem. *Trends Pharmacol. Sci.* 4, 450–454.
- Chou, T.-C., Talalay, P., 1984. Quantitative analysis of dose-effect relationships: the combined effects of multiple drugs or enzyme inhibitors. *Adv. Enzyme Regul.* 22, 27–55.
- Chou, T., Martin, N., 2005. *CompuSyn For Drug Combinations: PC Software and User's guide: a Computer Program For Quantitation of Synergism and Antagonism in Drug combinations, and the Determination of IC50 and ED50 and LD50 Values.* ComboSyn Inc, Paramus, (NJ).
- Cohen, G.M., 1997. Caspases: the executioners of apoptosis. *Biochem. J.* 326, 1–16.
- D'Orazio, J., Jarrett, S., Amaro-Ortiz, A., Scott, T., 2013. UV radiation and the skin. *Int. J. Mol. Sci.* 14, 12222–12248.
- Darzynkiewicz, Z., Juan, G., 1997. *Current Protocols in Cytometry.* In: Robinson, J.P. (Ed.), J. Wiley & Sons, New York 7.5. 1–7.5. 24.
- Dufau, I., Frongia, C., Sicard, F., Dediuet, L., Cordelier, P., Ausseil, F., Ducommun, B., Valette, A., 2012. Multicellular tumor spheroid model to evaluate spatio-temporal dynamics effect of chemotherapeutics: application to the gemcitabine/CHK1 inhibitor combination in pancreatic cancer. *BMC Cancer* 12, 15.
- Elmore, S., 2007. Apoptosis: a review of programmed cell death. *Toxicol. Pathol.* 35, 495–516.
- Franken, N.A., Rodermond, H.M., Stap, J., Haveman, J., Van Bree, C., 2006. Clonogenic assay of cells in vitro. *Nat. Protocol* 1, 2315–2319.
- Fruehauf, J.P., Meyskens, F.L., 2007. Reactive oxygen species: a breath of life or death. *Clin. Cancer Res.* 13, 789–794.
- Girola, N., Figueiredo, C.R., Farias, C.F., Azevedo, R.A., Ferreira, A.K., Teixeira, S.F., Capello, T.M., Martins, E.G., Matsuo, A.L., Travassos, L.R., 2015. Camphene isolated from essential oil of *Piper cernuum* (Piperaceae) induces intrinsic apoptosis in melanoma cells and displays antitumor activity in vivo. *Biochem. Biophys. Res. Comm.* 467, 928–934.
- Ho, W.Y., Yeap, S.K., Ho, C.L., Rahim, R.A., Alitheen, N.B., 2012. Development of multicellular tumor spheroid (MCTS) culture from breast cancer cell and a high throughput screening method using the MTT assay. *PLoS One* 7, e44640.
- Jasinski, P., Zwolak, P., Terai, K., Dudek, A.Z., 2008. Novel Ras pathway inhibitor induces apoptosis and growth inhibition of K-ras-mutated cancer cells in vitro and in vivo. *Transl. Res.* 152, 203–212.
- Kumar, A., Malik, F., Bhushan, S., Sethi, V.K., Shahi, A.K., Taneja, S.C., Qazi, G.N., Singh, J., 2008. An essential oil and its major constituent isomenthylolol induce apoptosis by increased expression of mitochondrial cytochrome c and apical death receptors in human leukaemia HL-60 cells. *Chem. Biol. Interact.* 171, 332–347.
- Lau, A.T., Wang, Y., Chiu, J.F., 2008. Reactive oxygen species: current knowledge and applications in cancer research and therapeutic. *J. Cell. Biochem.* 104, 657–667.
- Lazebnik, Y.A., Kaufmann, S.H., Desnoyers, S., Poirier, G., Earnshaw, W., 1994. Cleavage of poly (ADP-ribose) polymerase by a proteinase with properties like ICE. *Nature* 371, 346–347.
- Legault, J., Pichette, A., 2007. Potentiating effect of  $\beta$ -caryophyllene on anticancer activity of  $\alpha$ -humulene, isocaryophyllene and paclitaxel. *J. Pharm. Pharmacol.* 59, 1643–1647.
- Lehman, T.A., Modali, R., Boukamp, P., Stanek, J., Bennett, W.P., Welsh, J.A., Metcalf, R.A., Stampfer, M.R., Fusenig, N., Rogan, E.M., 1993. p53 mutations in human immortalized epithelial cell lines. *Carcinogenesis* 14, 833–839.
- Liu, X., Kim, C.N., Yang, J., Jemmerson, R., Wang, X., 1996. Induction of apoptotic program in cell-free extracts: requirement for dATP and cytochrome c. *Cell* 86, 147–157.
- Low, D., Rawal, B., Griffin, W., 1974. Antibacterial action of the essential oils of some Australian Myrtaceae with special references to the activity of chromatographic fractions of oil of *Eucalyptus citriodora*. *Planta Med.* 26, 184–189.
- Madan, V., 2009. Environmental risk factors for non-melanoma skin cancers. In: Jemec, G.B.E., Kemeny, L., Miecz, D. (Eds.), *Non-Surgical Treatment of Keratinocyte Skin Cancer.* Springer Berlin Heidelberg, Berlin, Heidelberg, pp. 39–50.
- Maddodi, N., Setaluri, V., 2008. Role of UV in cutaneous melanoma. *Photochem. Photobiol.* 84, 528–536.
- McGuire, J.F., Norman, N.G., Dyson, S., 2009. Nonmelanoma skin cancer of the head and neck I: histopathology and clinical behavior. *Am. J. Otolaryngol.* 30, 121–133.
- Mosmann, T., 1983. Rapid colorimetric assay for cellular growth and survival: application to proliferation and cytotoxicity assays. *J. Immunol. Methods* 65, 55–63.
- Moungjaroen, J., Nimmannit, U., Callery, P.S., Wang, L., Azad, N., Lipipun, V., Chanvorachote, P., Rojanasakul, Y., 2006. Reactive oxygen species mediate caspase activation and apoptosis induced by lipoic acid in human lung epithelial cancer cells through Bcl-2 down-regulation. *J. Pharmacol. Exp. Ther.* 319, 1062–1069.
- Oltval, Z.N., Milliman, C.L., Korsmeyer, S.J., 1993. Bcl-2 heterodimerizes in vivo with a conserved homolog, Bax, that accelerates programmed cell death. *Cell* 74, 609–619.
- Onawunmi, G.O., Yisak, W.-A., Ogunlana, E., 1984. Antibacterial constituents in the essential oil of *Cymbopogon citratus* (DC.) Stapf. *J. Ethnopharmacol.* 12, 279–286.
- Ortonne, J.P., 2002. From actinic keratosis to squamous cell carcinoma. *Br. J. Dermatol.* 146, 20–23.
- Park, D.J., Nakamura, H., Chumakov, A.M., Said, J.W., Miller, C.W., Chen, D.L., Koeffler, H.P., 1994. Transactivational and DNA binding abilities of endogenous p53 in p53 mutant cell lines. *Oncogene* 9, 1899–1906.
- Patel, T., Gores, G.J., Kaufmann, S.H., 1996. The role of proteases during apoptosis. *FASEB J.* 10, 587–597.
- Pathania, A.S., Guru, S.K., Verma, M., Sharma, C., Abdullah, S.T., Malik, F., Chandra, S., Katoch, M., Bhushan, S., 2013. Disruption of the PI3K/AKT/mTOR signaling cascade and induction of apoptosis in HL-60 cells by an essential oil from *Monarda citriodora*. *Food Chem. Toxicol.* 62, 246–254.
- Pavithra, P.S., Mehta, A., Verma, R.S., 2017. Induction of apoptosis by essential oil from *P. missionis* in skin epidermoid cancer cells. *Phytomedicine.* <https://doi.org/10.1016/j.phymed.2017.11.004>.
- Prasad, S., Ravindran, J., Sung, B., Pandey, M.K., Aggarwal, B.B., 2010. Garcinol potentiates TRAIL-induced apoptosis through modulation of death receptors and anti-apoptotic proteins. *Mol. Cancer Ther.* 9, 856–868.
- Ribble, D., Goldstein, N.B., Norris, D.A., Shellman, Y.G., 2005. A simple technique for quantifying apoptosis in 96-well plates. *BMC Biotechnol.* 5, 12.
- Rodust, P., Stockfleth, E., Ulrich, C., Leverkus, M., Eberle, J., 2009. UV-induced squamous cell carcinoma—a role for antiapoptotic signalling pathways. *Br. J. Dermatol.* 161, 107–115.
- Rogers, H.W., Weinstock, M.A., Harris, A.R., Hinckley, M.R., Feldman, S.R., Fleischer, A.B., Coldiron, B.M., 2010. Incidence estimate of nonmelanoma skin cancer in the United States, 2006. *Arch. Dermatol.* 146, 283–287.
- Shukla, Y., Prasad, S., Tripathi, C., Singh, M., George, J., Kalra, N., 2007. In vitro and in vivo modulation of testosterone mediated alterations in apoptosis related proteins by [6]-gingerol. *Mol. Nutr. Food Res.* 51, 1492–1502.
- Sun, S.-Y., Hail Jr, N., Lotan, R., 2004. Apoptosis as a novel target for cancer chemoprevention. *J. Natl. Cancer Inst.* 96, 662–672.
- Suzuki, T., Ezure, T., Ishida, M., 1998. Biochemistry: synergistic effects of some pairs of antioxidants and related agents on mouse leukaemia L5178Y cell growth in-vitro. *J. Pharm. Pharmacol.* 50, 1173–1177.
- Tallarida, R.J., 2006. An overview of drug combination analysis with isobolograms. *J. Pharmacol. Exp. Ther.* 319, 1–7.
- Tewari, M., Quan, L.T., O'Rourke, K., Desnoyers, S., Zeng, Z., Beidler, D.R., Poirier, G.G., Salvesen, G.S., Dixit, V.M., 1995. Yama/CPP32 $\beta$ , a mammalian homolog of CED-3, is a CrmA-inhibitable protease that cleaves the death substrate poly (ADP-ribose) polymerase. *Cell* 81, 801–809.
- Wang, X., 2001. The expanding role of mitochondria in apoptosis. *Genes Dev.* 15, 2922–2933.
- Wood, E., Bladon, P., 1985. *The Human Skin (Studies in Biology Series, No. 164).* Edward Arnold, London.
- Yamaguchi, M., Levy, R.M., 2016. The combination of  $\beta$ -caryophyllene, baicalin and catechin synergistically suppresses the proliferation and promotes the death of RAW267.4 macrophages in vitro. *Int. J. Mol. Med.* 38, 1940–1946.
- Zamzami, N., Marchetti, P., Castedo, M., Decaudin, D., Macho, A., Hirsch, T., Susin, S.A., Petit, P.X., Mignotte, B., Kroemer, G., 1995. Sequential reduction of mitochondrial transmembrane potential and generation of reactive oxygen species in early programmed cell death. *J. Exp. Med.* 182, 367–377.